Title

Investigation of Arrays of Two-Dimensional High-T_C SQUIDs for Optimization of Electrical Properties

Journal

IEEE Transactions on Applied Superconductivity, 29(5)

ISSN

1051-8223

Authors

Cho, Ethan Y

Zhou, Yuchao W

Khapaev, Mikhail M

et al.

Publication Date

2019-08-01

DOI

10.1109/tasc.2019.2904481

Peer reviewed

Investigation of Arrays of Two-Dimensional High-T_C SQUIDs for Optimization of Electrical Properties

Ethan Y. Cho, *Member, IEEE*, Yuchao W. Zhou, Mikhail M. Khapaev, and Shane A. Cybart, *Member, IEEE*

***Abstract*—In this work, we investigate two-dimensional arrays of high-T_C superconducting quantum interference devices (SQUIDs) for optimization of their electrical transport characteristics. Specifically, we look at devices with different electrode configurations in between the series segments to gain insight into how the array spacing, in the direction of the bias current, affects the voltage magnetic field characteristics. Our results suggest that for spacing dimensions greater than the penetration depth interactions are minimal. Furthermore, comparisons of voltage field characteristics reveal higher modulation voltages and narrower peaks with as the numbers of SQUIDs in the parallel direction increases from 1 to 6. For larger numbers of SQUIDs in parallel greater than six little change is observed. These results suggest a pathway to SQUID array scaling for very large numbers of SQUIDs within in a small area.**

***Index Terms*—SQUID, inductance, large scale.**

I. Introduction

ARRAYS of superconducting quantum interference devices (SQUIDs) may be able to provide improvements to the dynamic range, bandwidth and linearity of SQUID-based magnetometers [1]–[5]. This is particularly important for small signal detection applications, such as broadband RF antenna, operating unshielded or in the presence of large background interference [6]–[9]. These applications require a very large number of SQUIDs or equivalently Josephson junctions with uniform reproducible parameters. Ion damage high-T_C Josephson junctions [10] are ideal for this purpose because very large numbers of freely positional junctions are possible with 10% uniformity [11] and excellent temporal stability [12]. Large arrays of ion damage junctions previously demonstrated, exhibited much smaller voltage modulations than those predicted from the sum of the junction I_CR products [10], [11]. A computational modeling study suggested that this could be related to mutual interactions between adjacent SQUID loops [13]. In this manuscript, we take a closer look at these interactions with an experimental comparison of spatially extended and close-packed SQUID arrays for insight into how geometry affects the current distribution and voltage response to determine the potential scalability of these devices.

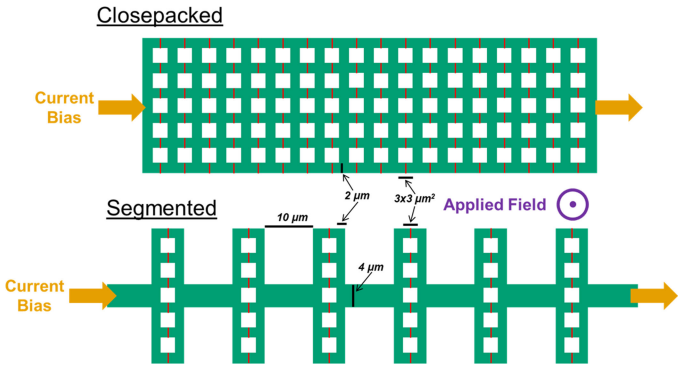

Fig. 1. Compact and extended array geometries for the devices used in this study. The number of SQUIDs connected in parallel for each segment was varied between 1 and 9 (5 is illustrated here). Both geometries contained 1000 series segments.

II. Experiment

Two types of SQUID array layouts developed for this experiment are shown in Fig. 1. In the close packed geometry, the devices are placed as close as possible within the bounds of the process critical dimension of 2 μm. In between each segment in the series direction the interconnecting electrode spans the entire width of the array. Whereas, in the extended geometry, an additional electrode several microns long is placed in the center in-between adjacent series segments. The choice of this extension was intended to reduce the mutual inductance between each segment. Arrays in both configurations were fabricated with the number of SQUIDs connected in parallel ranging from 1 to 9. All devices have identical segments connected in series.

Arrays were fabricated using the following process. A 150-nm thick YBCO thin film was deposited on a cerium oxide buffered 4-inch r-plane sapphire wafer by reactive coevaporation [14].

Manuscript received October 30, 2018; accepted February 7, 2019. Date of publication March 12, 2019; date of current version April 26, 2019. This work was supported in part by DOE, in part by the Air Force Office of Scientific Research under Grant FA955015-1-0218, in part by the National Science Foundation under Grant 1664446, in part by the Office of Naval Research, in part by the National Institutes of Health under Contract j1R43EB023147-01, and in part by the University of California, Office of the President Multicampus Research Programs and Initiatives under Award 009556-002. *(Corresponding author: Shane A. Cybart.)*

E. Y. Cho and Y. W. Zhou are with the Department of Mechanical Engineering, University of California, Riverside Riverside, CA 92521 USA (e-mail: eycho@ucr.edu; yzhou045@ucr.edu).

S. A. Cybart is with the Department of Mechanical Engineering, University of California, Riverside Riverside, CA 92521 USA, and also with the Material Science and Engineering Program, University of California, Riverside, Riverside, CA 92521 USA (e-mail: cybart@ucr.edu).

M. M. Khapaev is with the Department of Numerical Methods, Lomonosov Moscow State University, VMK, 119992 Moscow, Russia (e-mail: mkhapaev@gmail.com).

Color versions of one or more of the figures in this paper are available online at http://ieeexplore.ieee.org.

Digital Object Identifier 10.1109/TASC.2019.2904481

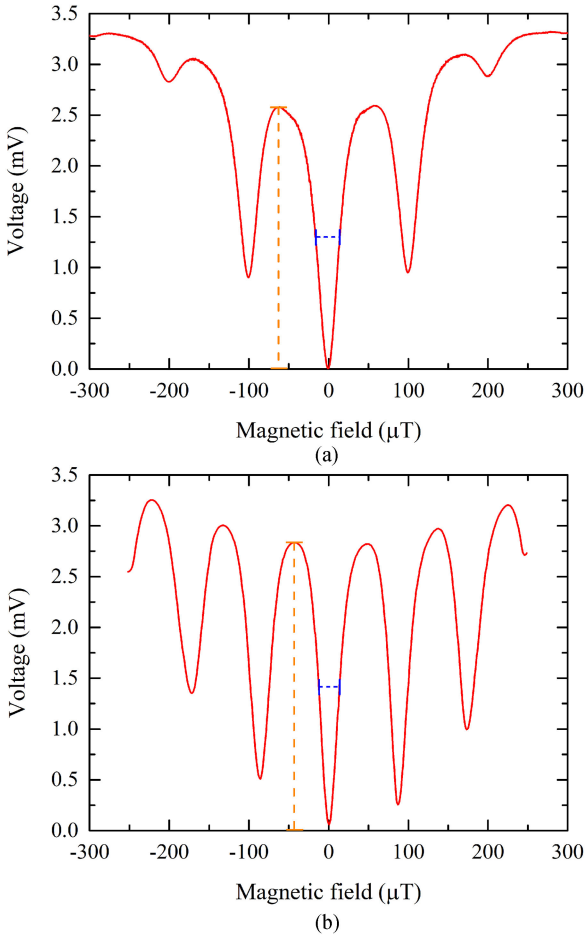

Fig. 2. Voltage-field characteristics of a (a) close packed (measured at 49 K) and (b) extended (measured at 45 K) array with eight SQUIDs in parallel and 1000 segments in series. Data were shifted by 5.2 mV (a) and 31.4 mV (b) for clarity. The slight difference in field period and shape of the voltage modulation are due to the different amounts of flux focusing from the electrodes.

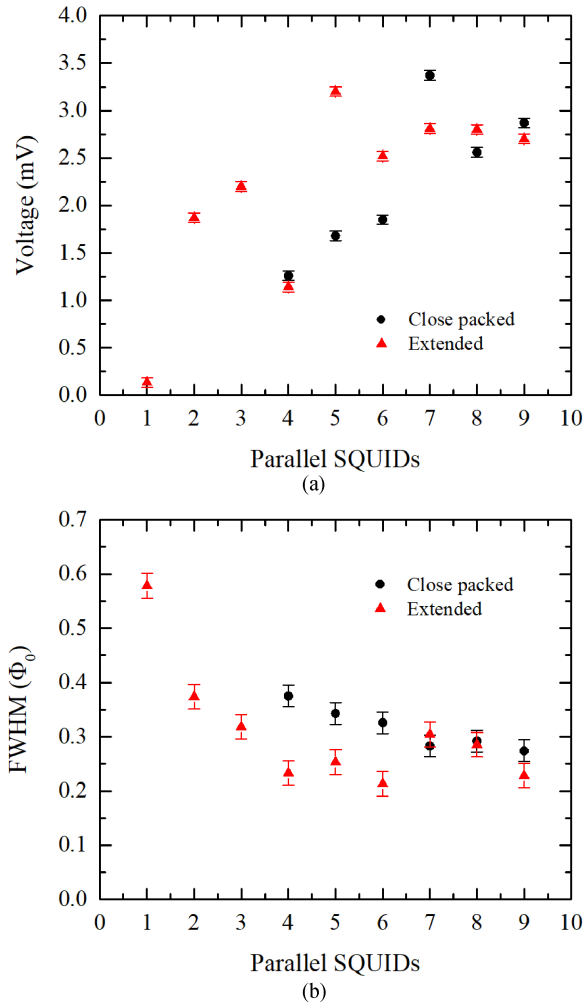

Fig. 3. (a) Maximum voltage modulation taken at different temperatures for different number of SQUIDs in parallel. (b) SQUID oscillation peak width as a function of different SQUIDs in parallel, the red indicates close packed array while the blue dots are extended arrays.

A subsequent 200-nm thick layer of gold was thermally evaporated *in-situ*. Electrodes were patterned into both layers using photolithography and argon ion milling. A subsequent lithography and KI-I-etch was used to pattern the gold contact layer. An ion implantation mask consisting of 800 nm-thick photoresist, 25 nm-thick germanium, and 100 nm of polymethylmethacrylate (PMMA) was constructed on top of the electrodes. Electron beam lithography with a Vistec VB6 100 keV nanowriter was used to expose 25-nm wide lines in the PMMA in the regions intended for Josephson junctions. After development the pattern was transferred into the underlying germanium layer using an HBr reactive ion etch. Subsequently, a second oxygen reactive ion etch was performed to transfer the pattern into the resist layer thereby forming a high aspect ratio implantation mask. The process is explained in a previous publication [15]. Last, the wafer was irradiated with 200 keV neon ions with a dose of 2×10^{13} ions/cm^2 to disorder the underlying YBCO film causing a reduction in T_C to form weak link Josephson junctions.

The implanted devices were diced and measured in a pumped liquid nitrogen cryostat for measurements in the temperature range 45 K to 77 K and a helium cryostat for lower temperatures. A layer of μ-metal sheidling and Bi-2223 superconductor shield were added to exclude external magnetic field. For testing, a DC bias current was driven through the array and voltage as a function of magnetic field *V-B* was measured over a wide range of temperature. The temperature and current bias that produced the largest voltage response was determined to optimize the characteristics for comparison to one another. We found a temperature spread in these optimum working points to be approximately 10 K which we attribute to process variations. Defects in the patterning prevented characterization of the close packed arrays with 1, 2, and 3 SQUIDs in parallel. Representative *V-B* for both geometries are shown in Fig. 2. Fig. 2(a) shows *V-B* of an 8 $\times$ 1000 close packed array optimally biased at 84 μA with voltage modulation of 2.56 mV and a maximum slope of 90 μV/μT. The SQUID oscillation period is 88 μT and full width at half maximum (FWHM) is 30.9 μT.

Similarly, Fig. 2(b) shows *V-B* of an extended array optimally biased at 193 μA with voltage modulation of 2.8 mV and the slope of 118 μV/μT. The SQUID oscillation period is 100 μT

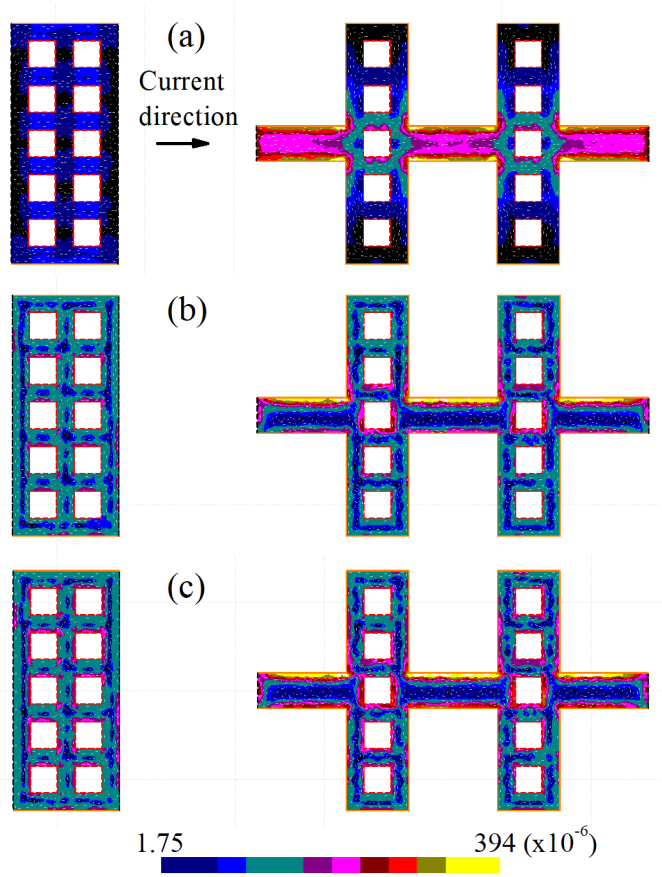

Fig. 4. 3D-MLSI simulation of current distribution of a close packed array and an extended array with (a) five SQUIDs in parallel and no external field, (b) magnetic field parameter of 0.5, and (c) 1 and current uniformly enters from the whole edge on the left. The color scale indicates a range from 1.75×10^{-6} to 394×10^{-6}.

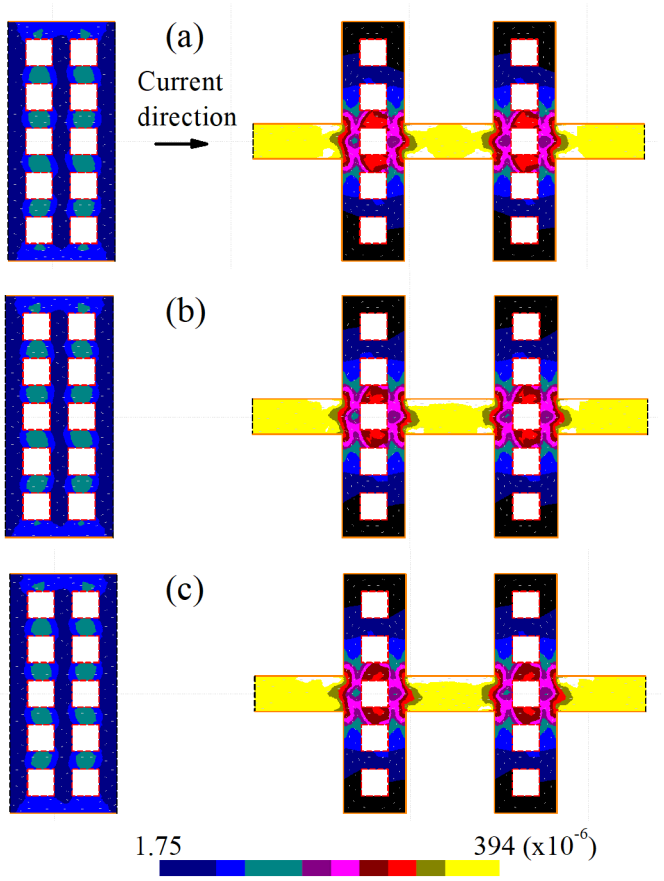

Fig. 5. 3D-MLSI simulation of current distribution of a close packed array and a extended array using the same condition as Fig. 4 with hole dimension reduced to 100 nm such that is is much less than λ. The color scale indicates a range from 1.75×10^{-6} to 394×10^{-6}.

with FWHM of 27.1 μT. The peak of the modulation voltage (V_P) was determined for the central peak of each array along with its FWHM as shown in Fig. 2.

Fig. 3(a) shows V_P as a function of the number of SQUIDs connected in parallel for both the close packed and extended geometries. We observe an increase in V_P with increasing parallel SQUID number up to approximately 6 SQUIDs, with little change for higher numbers. Furthermore, there is no measurable difference for the two device geometries.

Similarly, FWHM (normalized to the flux quantum) is plotted in Fig. 3(b). Narrowing of the central peak is quite evident as the numbers of SQUIDs increase from 1 to 6 but as in the previous case little change is noted at higher numbers. Furthermore the different electrode geometries show very similar results.

III. Discussion

To gain insight into our results we simulated the array segments using 3D-MLSI inductance simulation software for multi-layered circuits [16], [17]. The approach is based on the London equations written for the so-called stream function instead of electric current. A finite element method has been used for fast and precise calculations. For our particular simulations, we initialize the simulation with penetration depth $\lambda = 200$ nm, a bias current of 1 μA, and a triangular mesh consisting of 3654 pieces. We remark that this simulation does not take into account the presence of the resistances from the Josephson junctions. However, we believe the results are valid for studying the distributions of the supercurrents below the critical current of the array. Fig. 4(a)-(c) shows simulations for both geometries with applied flux $\Phi = 0, 1/4$ and 1/2 Φ_0 respectively. The countours depict the pathways of the circulating currents and the color scale indicates a range from 1.75×10^{-6} to 394×10^{-6}.

In the case of zero applied flux (Fig. 4(a)) current is concentrated in the center of the segment but as applied flux increases it redistributes across the SQUIDs evenly. With the exception of the centrally located SQUID, the circulating currents for both geometries are quite similar. We attribute this to be due to the fact that the electrodes are much larger than the superconducting penetration depth. To test this reasoning, we simulated a hypothetical device with critical features of 100 nm for both holes and electrodes which is smaller than the penetration depth of 200 nm. Fig. 5(a)–(c) shows simulations for both scaled down geometries with applied flux $\Phi = 0, 1/4$ and $1/2\Phi_0$ respectively. In contrast to the larger devices the nanoscale devices are strikingly different. All of the close packed arrays show a uniform current distribution whereas the extended geometry shows a very high current density at the electrode that is independent of applied

flux. At these smaller dimensions array geometry is very important and needs to be carefully considered for optimization of performance variables.

IV. Conclusion

In conclusion, we experimentally investigated two types of SQUID array geometry for optimization of closely packed geometries. No measurable difference was observed in the voltage response of our experimental arrays. While the critical dimensions of our devices were only 2 μm, simulations suggest that they are much larger than the penetration of the shielding currents between the segments, as the current density only changes rapidly near the edges. This result suggests that very aggressive scaling can be utilized to place larger numbers of SQUIDs into a smaller compact sensor with little degradation in performance. Assuming a spacing of 2λ (500 nm) between junctions, 2 μm-wide junction and 2λ pitch in a meander pattern, the junction density of this technology can be up to 10^8 cm^{-2}.

Furthermore, simulations of arrays with critical dimensions (CD) of 100 nm (CD $\ll \lambda_L$), reveal current crowding can occur at the electrodes, whereas in the close packed geometry the current remains evenly distributed. How these differences in current translate into the properties of *V-B* characteristics is an open question and merits further study at much smaller scales that is beyond the process technology used in this work. The use of helium ion direct-write SQUIDs [18], [19] could be utilized to realize these experiments for higher density arrays and new functionality.

Acknowledgment

The authors thank Bruce Harteneck and Erick Ulin-Avila for help with sample processing; Travis Wong for assistance in transport measurements, and Bob Dynes for enlightening discussions.

References

[1] E. E. Mitchell *et al.*, "2D SQIF arrays using 20 000 YBCO high R_n Josephson junctions," *Supercond. Sci. Technol.*, vol. 29, no. 6, 2016, Art. no. 06LT01.

[2] J. Oppenländer, C. Häussler, and N. Schopohl, "Non-ϕ_0-periodic macroscopic quantum interference in one-dimensional parallel Josephson junction arrays with unconventional grating structure," *Phys. Rev. B: Condens. Matter*, vol. 63, no. 2, 2000, Art. no. 024511.

[3] D. Drung, C. Hinnrichs, and H.-J. Barthelmess, "Low-noise ultra-high-speed DC SQUID readout electronics," *Supercond. Sci. Technol.*, vol. 19, no. 5, p. S235, 2006.

[4] M. E. Huber *et al.*, "DC SQUID series array amplifiers with 120 MHz bandwidth (corrected)," *IEEE Trans. Appl. Supercond.*, vol. 11, no. 2, pp. 4048–4053, Mar. 2001.

[5] V. K. Kornev, I. I. Soloviev, J. Oppenlaender, C. Haeussler, and N. Schopohl, "The oscillation linewidth and noise characteristics of a parallel superconducting quantum interference filter," *Supercond. Sci. Technol.*, vol. 17, no. 5, pp. S406–S409, 2004. [Online]. Available: http://stacks.iop.org/0953-2048/17/i=5/a=063

[6] V. K. Kornev, A. V. Sharafiev, I. I. Soloviev, N. V. Kolotinskiy, V. A. Scripka, and O. A. Mukhanov, "Superconducting quantum arrays," *IEEE Trans. Appl. Supercond.*, vol. 24, no. 4, Aug. 2014, Art. no. 1800606.

[7] S. Berggren *et al.*, "Development of 2-D bi-SQUID arrays with high linearity," *IEEE Trans. Appl. Supercond.*, vol. 23, no. 3, Jun. 2013, Art. no. 1400208.

[8] S. Ouanani *et al.*, "High-T_C superconducting quantum interference filters (SQUIFS) made by ion irradiation," *Supercond. Sci. Technol.*, vol. 29, no. 9, 2016, Art. no. 094002.

[9] O. V. Snigirev *et al.*, "Superconducting quantum interference filters as RF amplifiers," *IEEE Trans. Appl. Supercond.*, vol. 17, no. 2, pp. 718–721, Jun. 2007.

[10] S. A. Cybart, S. M. Anton, S. M. Wu, J. Clarke, and R. C. Dynes, "Very large scale integration of nanopatterned $YBa_2Cu_3O_{7-\delta}$ Josephson junctions in a two-dimensional array," *Nano Lett.*, vol. 9, no. 10, pp. 3581–3585, 2009.

[11] S. A. Cybart, S. M. Wu, S. M. Anton, I. Siddiqi, J. Clarke, and R. C. Dynes, "Series array of incommensurate superconducting quantum interference devices from $YBa_2Cu_3O_{7-\delta}$ ion damage Josephson junctions," *Appl. Phys. Lett.*, vol. 93, no. 18, 2008, Art. no. 182502.

[12] S. A. Cybart *et al.*, "Temporal stability of Y-Ba-Cu-O nano Josephson junctions from ion irradiation," *IEEE Trans. Appl. Supercond.*, vol. 23, no. 3, Jun. 2013, Art. no. 1100103.

[13] T. N. Dalichaouch, S. A. Cybart, and R. C. Dynes, "The effects of mutual inductances in two-dimensional arrays of Josephson junctions," *Supercond. Sci. Technol.*, vol. 27, no. 6, 2014, Art. no. 065006.

[14] H. Kinder, P. Berberich, W. Prusseit, S. Rieder-Zecha, R. Semerad, and B. Utz, "YBCO film deposition on very large areas up to 20 $\times$ 20 cm^2," *Physica C*, vol. 282, pp. 107–110, 1997.

[15] S. A. Cybart, P. Roediger, E. Ulin-Avila, S. M. Wu, T. J. Wong, and R. C. Dynes, "Nanometer scale high-aspect-ratio trench etching at controllable angles using ballistic reactive ion etching," *J. Vac. Sci. Technol., B*, vol. 31, no. 1, 2013, Art. no. 010604.

[16] M. M. Khapaev, M. Y. Kupriyanov, E. Goldobin, and M. Siegel, "Current distribution simulation for superconducting multi-layered structures," *Supercond. Sci. Technol.*, vol. 16, no. 1, pp. 24–27, 2002.

[17] M. M. Khapaev and M. Y. Kupriyanov, "Inductance extraction of superconductor structures with internal current sources," *Supercond. Sci. Technol.*, vol. 28, no. 5, 2015, Art. no. 055013. [Online]. Available: http://stacks.iop.org/0953-2048/28/i=5/a=055013

[18] E. Y. Cho *et al.*, "Yba2cu3o7- δ superconducting quantum interference devices with metallic to insulating barriers written with a focused helium ion beam," *Appl. Phys. Lett.*, vol. 106, no. 25, 2015, Art. no. 252601.

[19] E. Y. Cho, H. Li, J. C. Lefebvre, Y. W. Zhou, R. Dynes, and S. A. Cybart, "Direct-coupled micro-magnetometer with y-ba-cu-o nano-slit SQUID fabricated with a focused helium ion beam," *Appl. Phys. Lett.*, vol. 113, no. 14, Oct. 2018, Art. no. 162602. [Online]. Available: http://par.nsf.gov/biblio/10076662